

Dosimetry of the Electron Beams Generated by ‘LIAC’ for Intraoperative Radiation Therapy: Using GATE Monte Carlo Simulations

Maryam Amininejad¹, Seied Rabi Mahdavi², Elham Saeedzadeh^{1,*}

¹ Department of Radiation Medical Engineering, Science and Research Branch, Islamic Azad University, Tehran, Iran

² Radiation Biology Research Center, Medical Physics Department, Iran University of Medical Sciences, Tehran, Iran

*Corresponding author: Elham Saeedzadeh, Department of Radiation Medical Engineering, Science and Research Branch, Islamic Azad University, Tehran, Iran. Tel: +989192548678; Fax: +982144868407; E-mail: esaeedzadeh@srbiau.ac.ir

DOI: 10.30699/mci.5.4.524-1

Submitted: 23 May 2021

Revised: 17 Aug 2021

Accepted: 27 December 2021

e-Published: 28 December 2021

Keywords:

Intraoperative

Dosimetry

Electron Beam

GATE

Radiotherapy

Monte Carlo Method

Introduction: The dose distribution in the tumor bed and the neighboring tissue is an important issue in intraoperative radiation therapy (IORT). In the current study, a new software tool was developed to calculate and visualize the 2D and 3D dose distributions of the electron beams from the light intraoperative accelerator (LIAC) and validate the software through experimental measurements.

Methods: The Monte Carlo code ‘GATE’ was used to simulate the LIAC. Percentage depth dose curves (PDD) and transverse dose profiles (TDP) were calculated for all nominal energies in the water phantom, for the reference applicator.

Results: The dose distribution was defined in the form of isodose curves in the water phantom to study the volumetric and superficial changes of absorbed dose. There weren't significant differences between calculated and measured PDD curves and TDPs. R_{100} , R_{50} , R_{90} , R_p , and D_s values obtained from simulation were in good agreement with measurement. The maximum relative error was 8.6% which was related to R_{100} , due to the absence of charged particle equilibrium in the surface. As expected, the least error was related to R_{50} , making it the most common parameter in electron dosimetry.

Conclusions: The developed software is a basis to assess the dosimetric characteristics of all applicators and energy levels of the LIAC accelerator by calculating the 2D and 3D dose distribution during a proper calculation time. It can perform as a treatment planning system for IORT to calculate the absorbed dose of the clinical target volume and adjacent normal tissues which is not directly possible.

© 2021. Multidisciplinary Cancer Investigation

INTRODUCTION

Intraoperative radiation therapy (IORT) is a treatment technique to deliver a single high dose of radiation; normally more than 10 Gy (12-21Gy), to the tumor bed during surgery. The development of dedicated mobile accelerators for generating only electron beams shows the interest in using this method for the treatment of breast, rectal, gynecological, and prostate cancer during the past two decades [1-

5]. These portable accelerators can only produce electrons with energies up to 12 MeV [6-8]. The main difference between the mobile dedicated and conventional electron accelerators is the electron beam collimation system. In mobile accelerators, beam collimation is achieved through Poly Methyl Meth Acrylate (PMMA) applicators. The most common applicators are flat and beveled cylindrical

tubes in 3, 4, 5, 6, 7, 8, and 10 cm diameters [9]. Due to the lack of a commercial treatment planning system (TPS) for IORT systems, there is an increasing interest to evaluate the dose distribution in water phantom or even in the patient CT images during treatment, through Monte Carlo (MC) simulations [10, 11]. The dosimetric characteristics of the electron beam from IORT accelerators have been calculated in recent studies and were validated through experimental measurements. The dosimetric characteristics and water to air mass stopping power ratios were acquired by Monte Carlo simulations, for Novac7 and light intraoperative accelerator (LIAC) as two IORT accelerators; using BEAMnrc code and EBT radiochromic films [12]. Other studies also used BEAMnrc MC code to simulate a LIAC accelerator [8, 13-16]. To the best of our knowledge, no reports have been published yet on the development of software for the dosimetry of LIAC systems; using the GATE Monte Carlo code. The Gate provides adequate requirements to model and simulates the details of both LIAC head geometry and electron beams parameters.

The main aim of this study was to develop a novel software tool for the calculation and visualization of 2D and 3D dose distributions, based on GATE Monte Carlo simulations which could perform as a reliable TPS. Several physical assessments and quality assurance measures have to be carried out before a new software for treatment planning could be clinically used. The developed software may be a basis to assess the dosimetric characteristics of all applicators and energy levels of the LIAC accelerator by calculating the 2D and 3D dose distribution in a water phantom during a proper calculation time. This software may be applied to calculate the 3D dose distribution in a patient specific voxel phantom, based on CT images of the patient. It could perform as a dedicated TPS for IOERT: using LIAC systems.

METHODS

Monte Carlo Simulations of LIAC

MC is considered to be the most accurate and detailed calculation method in radiotherapy to calculate the dose distribution, even in particular configurations, validation of TPS and evaluation of their intrinsic limitations, etc. In this study, the LIAC accelerator has been simulated; using Gate (V7_2) MC code. LIAC (SordinaS.p.A, Italy, 2003)

is a mobile electron accelerator specially designed for intraoperative radiotherapy. The electron energies of the LIAC used in this study are 6, 8, 10, and 12 MeV [17]. GATE simply takes into account the optimized source and geometric parameters and calculates the distant energy deposition in a voxel-based dosimetry approach [18]. The diameters of the cylindrical applicators usually range from 3 to 10 cm [9]. The flat electron applicator with a diameter of 10 cm was considered as the reference applicator for dose rate measurements and the ratio between the measured dose for a certain applicator and the dose of the 10 cm diameter applicator in the depth of maximum dose for each energy, was defined as the output factor (OF). However, for reference dosimetry, the dosimetric characteristics of the reference applicator were calculated; using MC simulations as well as measurements with a PTW Advanced Markus chamber. Table 1 shows the simulated geometry including the titanium exit window, aluminum scattering foil, monitor ion chambers, and applicator.

Table 1: The Main Components of the Accelerator Head Along With the Materials Used to Model Them in Gate Monte Carlo Simulations

LIAC components	Material
Titanium exit window	Titanium (Ti)
Scattering foil	Aluminum (Al)
Monitor unit chamber	Aluminum (Al), Air (AIR), Mylar (MYLAR)
Applicator	PMMA
Surrounding structures	PEEK

The ending of the applicator was placed perpendicularly on the surface of the water phantom. Source to surface distance (SSD) was considered as the distance between the scattering foil and the end of the applicator, which was equal to 713 mm. A55µm titanium foil was located at the exit window of the accelerating structure. The pencil beam electron source was located on the titanium exit window. The electron beam in the simulation was defined as a pencil beam source located on the titanium exit window. A Gaussian distribution was considered for the energy of the electrons with a full width at half maximum (FWHM) of 0.4 MeV. In most MC simulation codes, the cut-off energy was being used but in Gate MC code, the cut-off range

was defined in different regions of the simulation geometry to decrease the simulation time. In this study, the cut-off range for particle transport was set to 1 mm for Gamma and 0.2 mm for electrons, and also maximum step sizes in regions were set to 1 mm for all particles. The energy levels provided by the producer documentation, are nominal values of the electron beam energies. It is important to define an optimal value of electron beam energy in simulations to minimize the difference between measurements and simulations. To obtain the accurate energy for each nominal energy, about ten different simulations were performed. The energy of the electron beam was changed from ± 1 MeV with 0.5 MeV steps concerning the nominal energy. The spot size, emittance, and divergence angles were changed with 0.1 steps for all nominal energies to drive the best output. Different radiation components which lead to dose deposition such as scattered and direct electrons, Bremsstrahlung photons, photoelectric, Compton, gamma conversion, electron ionization, positron annihilation, and electron multiple scattering were considered.

3D Dose Calculation and Validation of the Software

MC approach needs an intensive computation, and typically takes days to calculate dose for one patient [19]; so reducing the calculation time is necessary. In this study, a high-performance computing (HPC) system, which has 200 computational cores with Xeon technology and 3 GHz speed, was employed to calculate the dose in a water phantom to provide a balance between the calculation time and accuracy of the calculation. For calculating the 3D-dose distribution in water, a voxelized water phantom was simulated with a dimension of $221 \times 221 \times 221$ mm³ and voxel size of $1 \times 1 \times 1$ mm³, respectively. To assure the statistical accuracy and decrease the statistical uncertainty in Monte Carlo simulations, as much as possible, the number of histories was set to 5×10^8 for each simulation. Percent depth dose (PDD) along the central axis of the electron beam and transverse dose profile (TDP) data of reference applicator were then exported from the simulation software and compared with our measurements for all LIAC accelerator energies. For validation of the MC simulation and determining the accurate deposited

energy in each voxel, calculated parameters such as the PDD and dose profile curves, were compared with experimental data, measured with the Advanced Markus ion chamber (PTW, Freiburg) in a water phantom. Advanced Markus (PTW) ion chamber is a waterproof plane-parallel ionization chamber with a sensitive cylindrical volume of 0.02 cm³ and a diameter of 5 mm. Gamma index was used to quantitatively assess the agreement rate between two dose distributions. However, the criterion of the difference between the dose and the distance to the agreement in the calculations for the gamma index was considered to be 3% and 3 mm, respectively. In the present study, calculations of gamma index were performed; using the MEPHYSTO (Verisoft 5.1 (5.1.0.35)) navigator software.

RESULTS

The simulated geometry of the LIAC accelerator and the produced electron beam is illustrated in Figure 1.

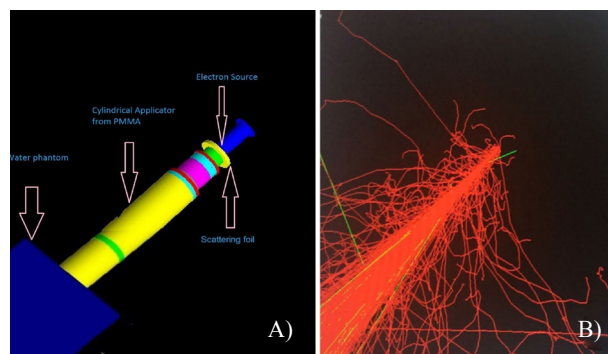


Figure 1: A Schematic Illustration

A) Light intraoperative accelerator (LIAC) accelerator and water phantom simulated with Gate and B) electron beam produced by LIAC

To drive the best estimation in MC simulation for different nominal energy of electron beams, several simulations were done and their PDDs are demonstrated in Figure 2.

PDD curves along with the central axis of the beam for each simulation in a water phantom were extracted from each dose matrices in all simulations. Three-dimensional dose distribution in a water phantom was calculated with a resolution of 1 mm. The uncertainty of absorbed dose in each voxel was less than 2% in target areas, for all energies. The calculated volumetric and superficial distribution of absorbed dose in a water phantom, along the Z-axis is illustrated in Figure 3. The dose distribution in

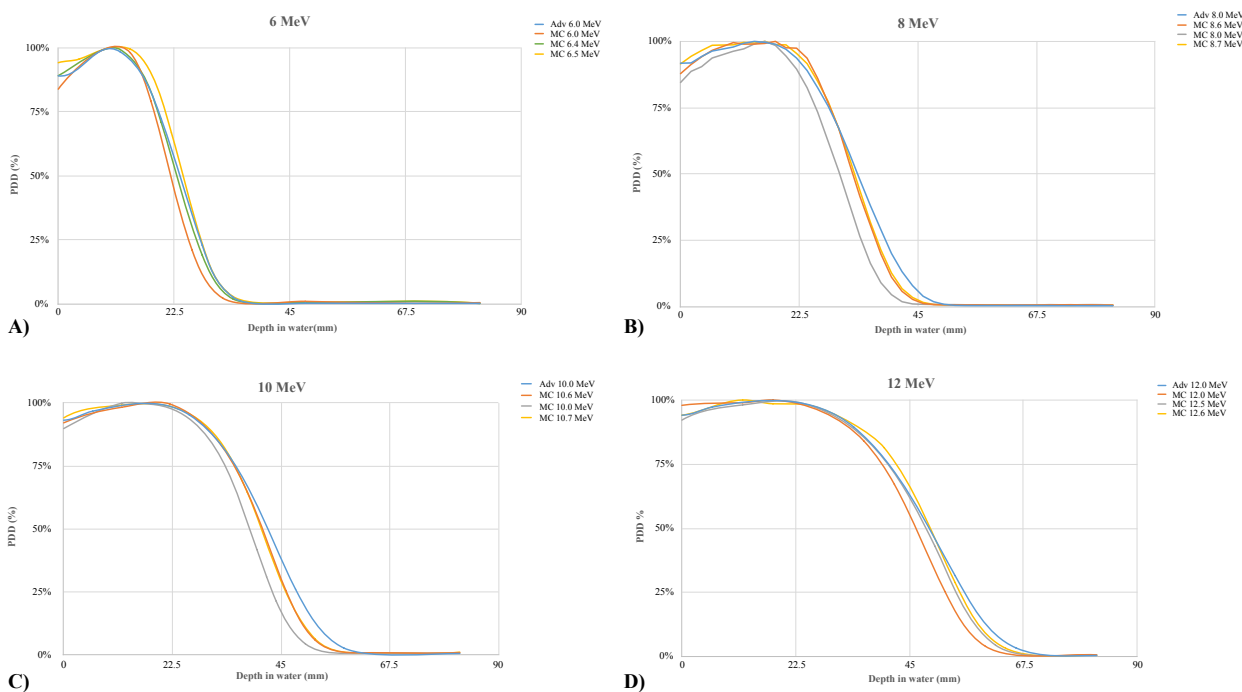


Figure 2: Percentage Depth Dose (PDDs) of Monte Carlo Simulation and Advanced Markus for Reference Applicator (10 cm diameter), for All Nominal Energies
 A), B), C), and D): Calculated PDDs for three simulations of electron beams compared with the measured PDD for the 6, 8 10, and 12 MeV nominal energies respectively.

the form of isodose curves in a water phantom was revealed for nominal energies of 6, 8, 10, and 12 MeV. The plotted graph is normalized (similar to the PDD curve) to the maximum dose value on the central axis in the central slice.

Figure 4 illustrates PDD curves along the central axis in the water phantom for the reference applicator (10 cm diameter) at 6, 8, 10, and 12 MeV nominal energy obtained from MC simulation and measurement. The parameters extracted from the

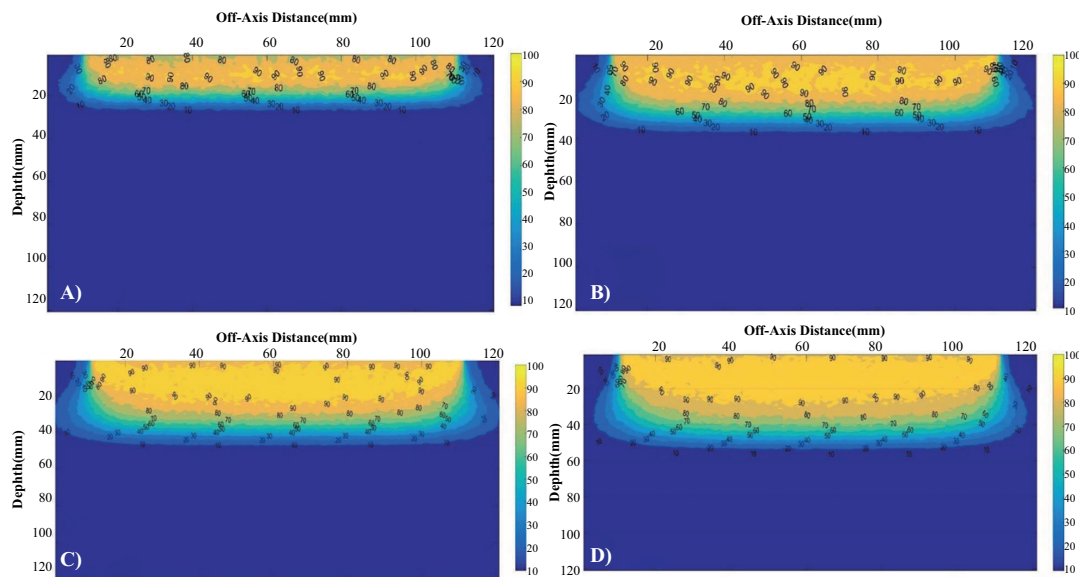


Figure 3: Isodose Curves in the Water Phantom in the Central Slice Which Is Normalized to the Maximum Dose on the Central Axis in Nominal Energies for Reference Applicator (10 cm diameter)
 A) 6 MeV; B) 8 MeV; C) 10 MeV; and D) 12 MeV

PDD curves included R_{100} , R_{50} , R_{90} , and R_p which represent the depth of maximum dose, 50%, 90%, and practical range in mm, respectively (Table 2). D_s , the percentage depth dose at the surface of water phantom in the reference applicator (10 cm diameter), is also given in Table 2. The relative error for R_{100} , R_{90} , R_{50} , R_p , and D_s between MC simulation and the Advanced Markus measurements in PDD curves is also shown in Table 2.

Figure 5 shows the dose profile curves in the water phantom for the reference applicator (10 cm diameter) and 6, 8, 10, and 12 MeV nominal energies. The profiles are acquired at d_{max} from MC simulations (calculated) and Advanced Markus measurements.

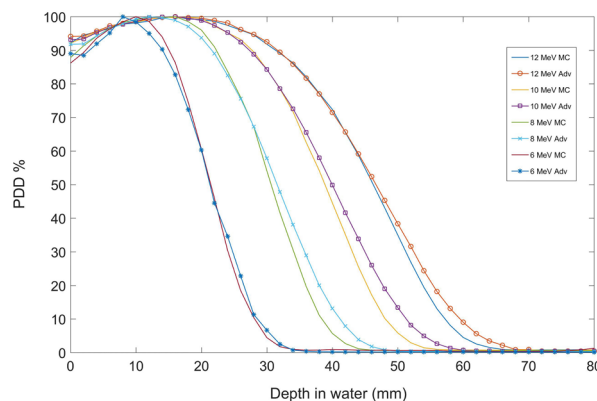


Figure 4: Percentage Depth Dose (PDD) Curves in the Water Phantom Obtained From MC Simulation (Calculated) and Advanced Markus (Measured) for the Reference Applicator (10 cm Diameter) at 6, 8, 10, and 12 MeV Nominal Energies

Table 2: Parameters Related to the Percentage Depth Dose (PDD) Curve Obtained From the Monte Carlo Simulation and the Ion Chamber, and Relative Error Between Each^a

Nominal Energy (MeV)	MC Simulation					Advanced Markus Measurement					Relative Error Between MC and Advanced Markus				
	R_{100} , mm	R_{90} , mm	R_{50} , mm	R_p , mm	D_s , %	R_{100} , mm	R_{90} , mm	R_{50} , mm	R_p , mm	D_s , %	R_{100} , mm	R_{90} , mm	R_{50} , mm	R_p , mm	D_s , %
6	10.0	14.5	21.4	28.0	86.0	9.2	14.0	21.2	28.6	89.0	8.6	3.5	0.9	-2.0	-3.3
8	14.0	22.2	30.6	39.0	87.0	13.0	22.0	31.5	41.0	91.0	7.6	0.9	-2.8	-4.8	-4.3
10	15.0	27.6	38.8	49.5	92.0	15.7	27.3	39.9	52.0	93.1	-4.4	1.0	-2.7	-4.8	-1.0
12	15.9	30.9	46.2	58.0	92.5	16.0	30.9	46.6	59.6	94.0	-0.6	0.0	-0.4	-2.6	-2.1

^a Abbreviations: D_s , percentage depth dose at the surface, R_{100} , depths of maximum dose; R_{90} , depths of 90% dose; R_{50} , depths of 50% dose, R_p , depths of practical range

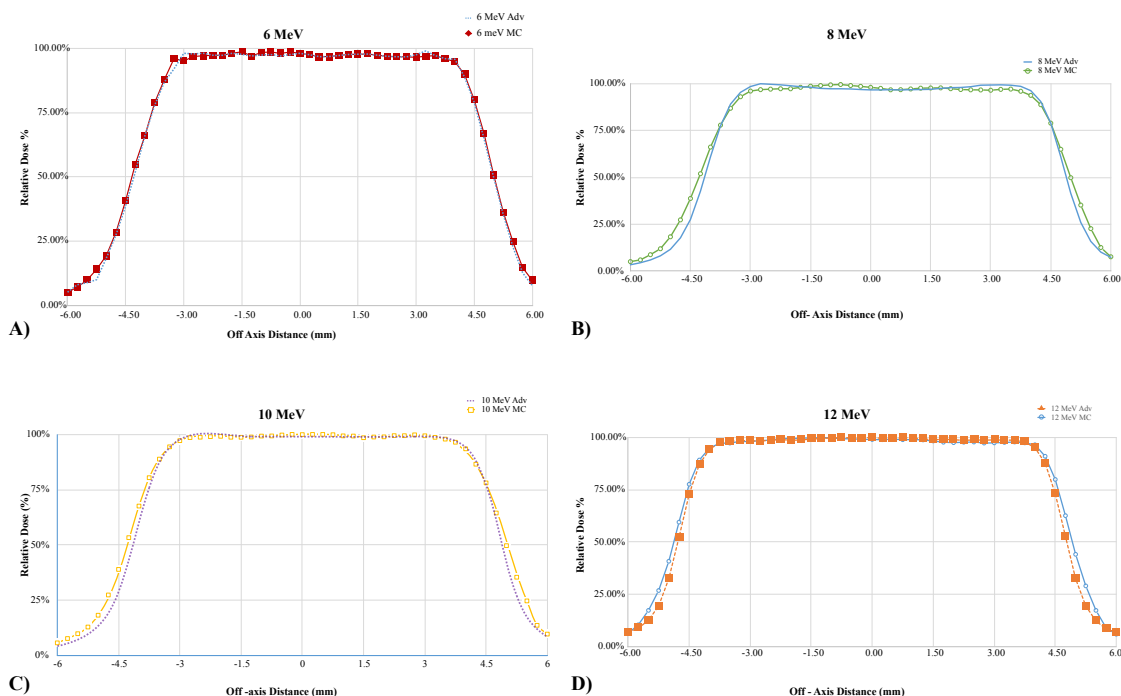


Figure 5: Measured and MC Transverse Dose Profiles (TDPs) at d_{max} for Different Electron Beam Nominal Energies and the Reference Applicator (10 cm diameter).

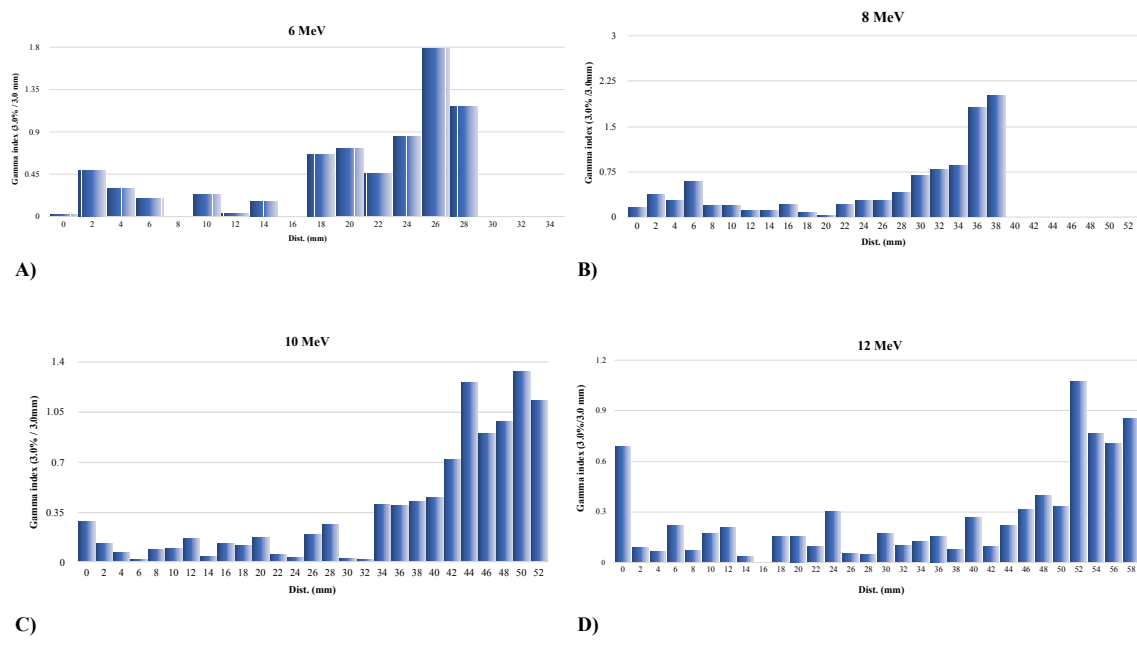


Figure 6: Histogram of Gamma Analysis for Percentage Depth Dose (PDD) Curves, Used for Validation of LIAC Simulation for References Applicator in All Nominal Energies

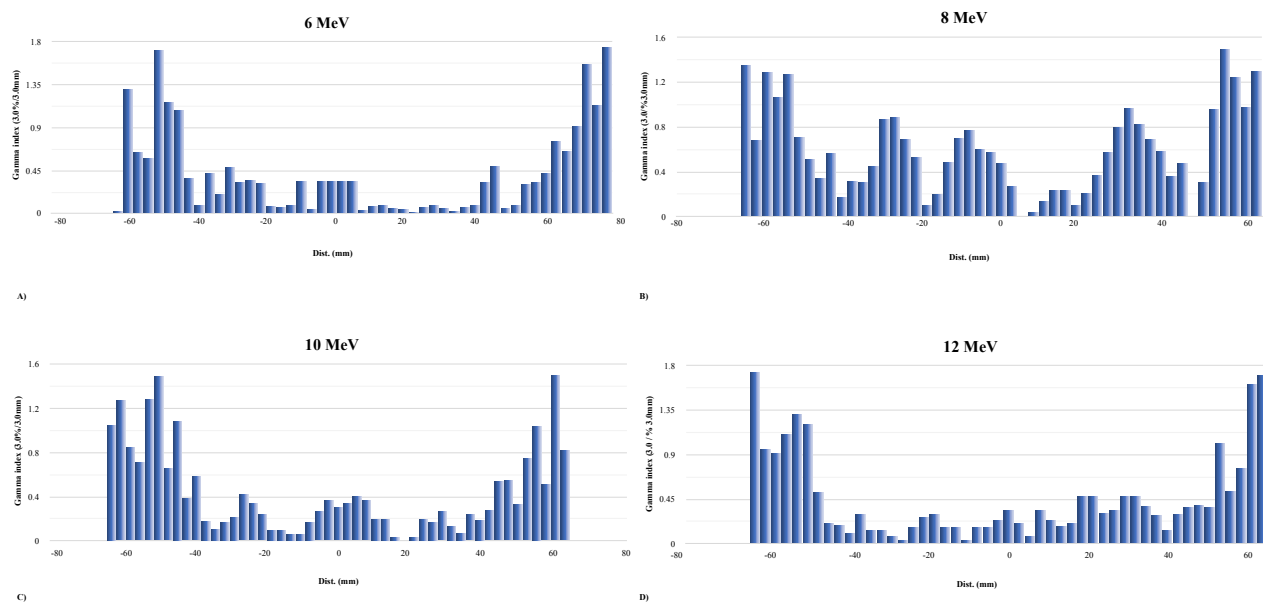


Figure 7: Histogram of Gamma Analysis for Transverse Dose Profiles (TDP) Curves, Used for Validation of LIAC Simulation for References Applicator in All Nominal Energies

As previously mentioned, the results of MC simulations were compared with measured data to ensure the accuracy of the parameters used in the simulation of LIAC and to validate the codes. The PDD and Dose profile curves were compared; using gamma analysis. Using a dose difference of 3% and distance to agreement of 3 mm, more than 90% of points, had a gamma index of less than 1. The results are presented in Figures 6 and 7. There was a good

agreement between calculated and experimental dose profiles and PDDs for all nominal energies.

DISCUSSION

A software tool was developed to calculate the dosimetric parameters of the electron beams produced by the LIAC mobile accelerator. To validate the simulations, the MC calculated results were compared with the experimental measurements and

[Downloaded from mcjournal.com on 2026-05-19]

[DOR: 20.1001.1.24764922.2021.5.4.3.3]

[DOI: 10.30699/mci.5.4.524-1]

were evaluated; using gamma analysis. Dosimetric characteristics such as PDD curves, dose profiles, and isodose curves of electron beams generated by LIAC, have been determined. Moreover, the surface dose was about 90% of d_{\max} for all nominal energies. Isodose curves indicate a rapid dose decrease beyond the depth of target volume and in areas with a transverse distance from the central axis [13, 14]. The relative error for R_{100} , R_{90} , R_{50} , R_p , and D_s between MC simulation and the Advanced Markus measurements in PDD curves are shown in Table 2. The maximum relative error was 8.6% which was related to R_{100} . The absence of charged particle equilibrium (CPE) in the surface may have led to errors in the experimental measurement of the surface dose. The least error is related to R_{50} , making it the most common parameter in electron dosimetry [4, 9]. Our result revealed that the gamma analysis for PDD curves indicates a good agreement between calculation results and measurements. The gamma index was less than one in most of the points, but in areas that were beyond the range of electrons, the statistical errors was increased due to the decreased number of electrons, both in MC simulations and in practical measurements. The other source of differences between calculated and measured data in PDD curves was the difference in dosimetry resolution. In this study, the dose measurement resolution was considered to be 1 mm in MC simulations and 2 mm in measurements. However, the discrepancy between the curves in deep points was not clinically significant, since the magnitude of dose in that area is almost zero. The results of this study, in terms of R_{100} , R_{90} , R_{50} , and R_p were compared with previous reports [12, 16]. In those studies, BEAMnrc MC code was used to model the LIAC head and electron beams and generate PDD curves and dose profiles. However, Advanced Markus ion chamber and Gafchromic film dosimetry were used to validate their simulations. The results of this study were in good agreement with those reported in the literature for most dosimetric parameters. However, in this study, R_{90} and R_{50} for 6 MeV electron beams are about 14 and 21.5 cm, respectively. These results are in good agreement with those reported by a previous study by Baghani, et al., [16], where these parameters were reported to be 17 and 25 cm [12]. This difference may be due to some differences in the energy of two systems for 6 MeV electrons or the resolution of dosimetry.

However, this issue needs further considerations to draw firm conclusions. Moreover, the dose profile curves show the variation of the dose across the radiation field at the maximum dose depth, d_{\max} , for all energies. The results of gamma analysis for TDP curves of all nominal energies for the reference applicator (10 cm) showed a good agreement between calculated and measured curves in most of the points. Moreover, the symmetry and flatness of electron beam dose profiles are nearly the same in MC simulation and measurement [9]. However, because of the lack of CPE in d_{\max} , there may be some errors in measuring the absorbed dose; using the chamber. This difference is more observed in the lateral areas of the field, because of the decrease in electron number which leads to increased statistical error both in MC simulations and measurements. MC simulation will improve the accuracy of beam dosimetry. The developed software in this study is dosimetrically well suited for IOERT and was proved to perform consistently. Also, a HPC system was used to reduce the simulation time up to five times. This approach serves as a basis for a dose planning tool. This planning tool provides relative dose distributions in three dimensions calculated in water for all applicators and energy levels. This software may provide a novel tool for the calculation and visualization of dose distributions proper dose calculation time of this software could be used to support and set up treatment planning.

ACKNOWLEDGMENTS

The authors are grateful to Dr. Golbarg Esmaeili and Dr. Hamidreza Baghani for their helpful suggestions.

CONFLICT OF INTEREST

The authors declare that they have no conflicts of interest.

ETHICS APPROVAL

None declared.

REFERENCES

1. Ciocca M, Pedroli G, Orecchia R, Guido A, Cattani F, Cambria R, et al. Radiation survey around a LIAC mobile electron linear accelerator for intraoperative radiation therapy. *J Appl Clin Med Phys*. 2009;10(2):131-8. DOI: [10.1120/jacmp.v10i2.2950](https://doi.org/10.1120/jacmp.v10i2.2950) PMID: [19458597](https://pubmed.ncbi.nlm.nih.gov/19458597/).
2. Soriani A, Felici G, Fantini M, Paolucci M, Borla O, Evangelisti G, et al. Radiation protection measurements around a 12 MeV mobile dedicated IORT accelerator. *Med Phys*.

- 2010;37(3):995-1003. DOI: [10.1118/1.3298012](https://doi.org/10.1118/1.3298012) PMID: [20384235](https://pubmed.ncbi.nlm.nih.gov/20384235/).
3. Beddar AS, Briere TM, Ouzidane M. Intraoperative radiation therapy using a mobile electron linear accelerator: field matching for large-field electron irradiation. *Phys Med Biol*. 2006;51(18):N331-7. DOI: [10.1088/0031-9155/51/18/N01](https://doi.org/10.1088/0031-9155/51/18/N01) PMID: [16953035](https://pubmed.ncbi.nlm.nih.gov/16953035/).
 4. Baghani HR, Aghamiri SM, Mahdavi SR, Robotjazi M, Zadeh AR, Akbari ME, et al. Dosimetric evaluation of Gafchromic EBT2 film for breast intraoperative electron radiotherapy verification. *Phys Med*. 2015;31(1):37-42. DOI: [10.1016/j.ejmp.2014.08.005](https://doi.org/10.1016/j.ejmp.2014.08.005) PMID: [25231546](https://pubmed.ncbi.nlm.nih.gov/25231546/).
 5. Schneider F, Bludau F, Clausen S, Fleckenstein J, Obertacke U, Wenz F. Precision IORT - Image guided intraoperative radiation therapy (igIORT) using online treatment planning including tissue heterogeneity correction. *Phys Med*. 2017;37:82-7. DOI: [10.1016/j.ejmp.2017.04.017](https://doi.org/10.1016/j.ejmp.2017.04.017) PMID: [28535919](https://pubmed.ncbi.nlm.nih.gov/28535919/).
 6. Mills MD, Fajardo LC, Wilson DL, Daves JL, Spanos WJ. Commissioning of a mobile electron accelerator for intraoperative radiotherapy. *J Appl Clin Med Phys*. 2001;2(3):121-30. DOI: [10.1120/jacmp.v2i3.2605](https://doi.org/10.1120/jacmp.v2i3.2605) PMID: [11602008](https://pubmed.ncbi.nlm.nih.gov/11602008/).
 7. Loi G, Domenietto M, Cannillo B, Ciocca M, Krengli M, Mones E, et al. Neutron production from a mobile linear accelerator operating in electron mode for intraoperative radiation therapy. *Phys Med Biol*. 2006;51(3):695-702. DOI: [10.1088/0031-9155/51/3/014](https://doi.org/10.1088/0031-9155/51/3/014) PMID: [16424589](https://pubmed.ncbi.nlm.nih.gov/16424589/).
 8. Iaccarino G, Strigari L, D'Andrea M, Bellesi L, Felici G, Ciccotelli A, et al. Monte Carlo simulation of electron beams generated by a 12 MeV dedicated mobile IORT accelerator. *Phys Med Biol*. 2011;56(14):4579-96. DOI: [10.1088/0031-9155/56/14/022](https://doi.org/10.1088/0031-9155/56/14/022) PMID: [21725139](https://pubmed.ncbi.nlm.nih.gov/21725139/).
 9. Baghani HR, Aghamiri SM, Mahdavi SR, Akbari ME, Mirzaei HR. Comparing the dosimetric characteristics of the electron beam from dedicated intraoperative and conventional radiotherapy accelerators. *J Appl Clin Med Phys*. 2015;16(2):5017. DOI: [10.1120/jacmp.v16i2.5017](https://doi.org/10.1120/jacmp.v16i2.5017) PMID: [26103175](https://pubmed.ncbi.nlm.nih.gov/26103175/).
 10. Pimpinella M, Andreoli S, De Angelis C, Della Monaca S, D'Arienzo M, Menegotti L. Output factor measurement in high dose-per-pulse IORT electron beams. *Phys Med*. 2019;61:94-102. DOI: [10.1016/j.ejmp.2019.04.021](https://doi.org/10.1016/j.ejmp.2019.04.021) PMID: [31151586](https://pubmed.ncbi.nlm.nih.gov/31151586/).
 11. Pascau J, Santos Miranda JA, Calvo FA, Bouche A, Morillo V, Gonzalez-San Segundo C, et al. An innovative tool for intraoperative electron beam radiotherapy simulation and planning: description and initial evaluation by radiation oncologists. *Int J Radiat Oncol Biol Phys*. 2012;83(2):e287-95. DOI: [10.1016/j.ijrobp.2011.12.063](https://doi.org/10.1016/j.ijrobp.2011.12.063) PMID: [22401923](https://pubmed.ncbi.nlm.nih.gov/22401923/).
 12. Righi S, Karaj E, Felici G, Di Martino F. Dosimetric characteristics of electron beams produced by two mobile accelerators, Novac7 and Liac, for intraoperative radiation therapy through Monte Carlo simulation. *J Appl Clin Med Phys*. 2013;14(1):3678. DOI: [10.1120/jacmp.v14i1.3678](https://doi.org/10.1120/jacmp.v14i1.3678) PMID: [23318376](https://pubmed.ncbi.nlm.nih.gov/23318376/).
 13. Robotjazi M, Tanha K, Mahdavi SR, Baghani HR, Mirzaei HR, Mousavi M, et al. Monte Carlo Simulation of Electron Beams produced by LIAC Intraoperative Radiation Therapy Accelerator. *J Biomed Phys Eng*. 2018;8(1):43-52. PMID: [29732339](https://pubmed.ncbi.nlm.nih.gov/29732339/).
 14. Mihailescu D, Borcia C. Monte Carlo simulation of the electron beams produced by a linear accelerator for intraoperative radiation therapy. *Rom Rep Phys*. 2014;66(1):61-74.
 15. Marrale M, Longo A, Russo G, Casarino C, Candiano G, Gallo S, et al. Dosimetry for electron Intra-Operative RadioTherapy: Comparison of output factors obtained through alanine/EPR pellets, ionization chamber and Monte Carlo-GEANT4 simulations for IORT mobile dedicate accelerator. *Nucl Instrum Methods Phys Res B: Beam Interactions with Materials and Atoms*. 2015;358:52-8. DOI: [10.1016/j.nimb.2015.05.022](https://doi.org/10.1016/j.nimb.2015.05.022).
 16. Adrich P, Hanke R, Kulczycka E, Kosiński K, Meglicki B, Misiarz A, et al. The IOERT IntraLine accelerator: the development, current state, and future plans. *Nukleonika*. 2016;61(1):3-9.
 17. Saeedzadeh E, Sarkar S, Abbaspour Tehrani-Fard A, Ay MR, Khosravi HR, Loudos G. 3D calculation of absorbed dose for 131I-targeted radiotherapy: a Monte Carlo study. *Radiat Prot Dosimetry*. 2012;150(3):298-305. DOI: [10.1093/rpd/ncr411](https://doi.org/10.1093/rpd/ncr411) PMID: [22069233](https://pubmed.ncbi.nlm.nih.gov/22069233/).
 18. Downes P, Yaikhom G, Giddy JP, Walker DW, Spezi E, Lewis DG. High-performance computing for Monte Carlo radiotherapy calculations. *Philos Trans A Math Phys Eng Sci*. 2009;367(1897):2607-17. DOI: [10.1098/rsta.2009.0028](https://doi.org/10.1098/rsta.2009.0028) PMID: [19451114](https://pubmed.ncbi.nlm.nih.gov/19451114/).
 19. Jia X, Ziegenhein P, Jiang SB. GPU-based high-performance computing for radiation therapy. *Phys Med Biol*. 2014;59(4):R151-82. DOI: [10.1088/0031-9155/59/4/R151](https://doi.org/10.1088/0031-9155/59/4/R151) PMID: [24486639](https://pubmed.ncbi.nlm.nih.gov/24486639/).